

# Carbothermic Reduction of Copper, Nickel, and Cobalt Oxides and Molybdates

N. V. Lebukhova and N. F. Karpovich

*Institute of Materials Science, Khabarovsk Scientific Center, Far East Division, Russian Academy of Sciences, Tikhookeanskaya ul. 153, Khabarovsk, 680042 Russia*

*e-mail: LNVI@yandex.ru*

Received July 30, 2007

**Abstract**—The carbothermic reduction of NiO, CoO, CuO, MoO<sub>3</sub>, and the MMoO<sub>4</sub> (M = Ni, Co, Cu) molybdates has been studied by thermogravimetry. The results demonstrate that the reactivity of the molybdates with solid carbon, the sequence of reduction reactions, and the composition of reaction intermediates are determined by the reactivity of the constituent oxides, which decreases in the order CuO > MoO<sub>3</sub> > NiO > CoO. The reaction intermediates in the reduction of CuMoO<sub>4</sub> are Cu<sub>6</sub>Mo<sub>5</sub>O<sub>18</sub> and Cu<sub>2</sub>Mo<sub>3</sub>O<sub>10</sub>, and those in the reduction of CoMoO<sub>4</sub> are Co<sub>2</sub>Mo<sub>3</sub>O<sub>8</sub> and CoMoO<sub>3</sub>. NiMoO<sub>4</sub> is reduced without oxide intermediates. The reactions of CuMoO<sub>4</sub> and NiMoO<sub>4</sub> with solid carbon lead to selective reduction of the molybdates to metals (Cu or Ni) and molybdenum oxides (MoO<sub>2</sub> and MoO<sub>3-x</sub>). In the reactions of NiMoO<sub>4</sub> and CoMoO<sub>4</sub> with CO gas, the metals are formed at comparable rates, which favors the formation of metal solid solutions, intermetallic phases, and mixed carbides.

**DOI:** 10.1134/S0020168508080207

## INTRODUCTION

In recent years, there has been increasing interest in the coreduction of metals in multicomponent oxide systems—not only for the extraction of elements from slags and mineral associations but also for the production of cermets. Intense scientific and technological interest has been centered on processes for the preparation of composite powders of hard tungsten alloys that would combine nanostructure with a highly homogeneous distribution of carbide phases and a metallic binder owing to the use of binary tungstate and molybdate systems as starting reagents and carbon as both a reductant and carbonizing reagent [1, 2]. The carbothermic reduction of mixed oxide systems is a multistep process which leads to the formation of various intermediate oxide phases and reduction products, depending on the nature of the starting reagents and synthesis conditions [3, 4]. Reduction annealing of binary molybdenum, tungsten, and copper oxides in hydrogen may follow a variety of reaction paths, which was found to influence the homogeneity of the metal distribution in the reduced phases and their composition and structure [4]. As shown in our earlier study of the phase formation sequence in reactions of nickel and cobalt tungstates with carbon [5], the reaction paths and, accordingly, the phase compositions of the reaction products differ significantly for CoWO<sub>4</sub> and NiWO<sub>4</sub>, which can be understood in terms of the reduction kinetics of the tungstates.

The purpose of this work was to establish the phase formation sequence in the carbothermic reduction of the MMoO<sub>4</sub> (M = Cu, Ni, Co) molybdates.

## EXPERIMENTAL

In our preparations, we used reagent- and analytical-grade oxides. CoMoO<sub>4</sub>, NiMoO<sub>4</sub>, and CuMoO<sub>4</sub> were prepared via coprecipitation from equimolar solutions of divalent-metal nitrates and sodium molybdate (Na<sub>2</sub>MoO<sub>4</sub>). The precipitates were calcined in air, first at 350 and then at 600°C, for a total of 2 h. The resultant powders were investigated in the as-prepared state or after grinding in a Petsch PM-400 planetary ball mill. The particle size distribution was evaluated using an Analysette 22 Comfort laser analyzer. The average particle diameter was determined as  $\bar{d} = \sum_i d_i n_i / \sum_i n_i$ , where  $\bar{d}$  is the average particle diameter,  $n$  is the number of particles in a given size range, and  $i$  is the number of size ranges. The reductant used was carbon black (RF State Standard GOST 12222-78). We used stoichiometric mixtures to obtain metals and also mixtures containing up to 50% excess carbon. The mixtures were prepared by grinding in an agate mortar. Reduction was carried out in flowing argon (15 l/h) during heating at a rate of 5°C/min or under quasi-isothermal conditions in the furnace of a MOM Q-1000 thermoanalytical system. The extent of reduction,  $\alpha$ , was evaluated from thermogravimetric (TG) curves as the ratio of the weight loss of the sample to the maximum possible gas

release, corresponding to the completion of the reaction and formation of the metal. Phase composition of reaction products was determined by x-ray diffraction (XRD) on a DRON-7 diffractometer with  $\text{CuK}_\alpha$  radiation.

## RESULTS AND DISCUSSION

The kinetics of reactions between oxides and carbon during the reduction process can be limited by various factors [6, 7]. In the absence of phase transitions and dissociation, the reduction of most metal oxides can be represented by a two-step scheme: in the first, slow step, the surface of particles reacts with solid carbon; in the second, faster step, the particle surface reacts with the CO resulting from the oxidation of carbon at temperatures above 750°C. Solid-state reactions between carbon and compounds having low vapor pressure (NiO, CuO,  $\text{Cu}_2\text{O}$ ) are only active in the first step of the reduction process. The forming barrier layer, consisting of the lower oxide or metal, prevents direct contact between the solid reactants. High reaction rates even in the first step of the reduction process can be insured by pairs of metal oxides that form via sublimation ( $\text{MoO}_3$ ,  $\text{WO}_3$ ,  $\text{V}_2\text{O}_5$ ) or dissociation ( $\text{Cu}_2\text{O}$ ,  $\text{Ag}_2\text{O}$ ,  $\text{MnO}_2$ ,  $\text{ZnO}$ ).

Figure 1 presents the TG data obtained at a constant heating rate of the furnace of the thermoanalytical system for reactions of carbon with CuO, CoO, NiO, and  $\text{MoO}_3$  powders preground in a planetary mill to roughly the same particle size,  $\bar{d} \approx 2\text{--}4\text{ }\mu\text{m}$ . The increase in reaction rate starting at 380°C (with a maximum at 525°C) in the initial stages of the reduction of CuO to the more stable oxide  $\text{Cu}_2\text{O}$  (Fig. 1, curve 1) is essentially insensitive to excess carbon and seems to be due to the solid-state reaction on the surface of the oxide particles. Raising the temperature increases  $\text{Cu}_2\text{O}$  dissociation: according to reference data [8],  $\log p_{\text{O}_2} = -46.5$  at 200°C and  $\log p_{\text{O}_2} = -8.8$  at 500°C, which insures the reduction of  $\text{Cu}_2\text{O}$  to copper metal (with a maximum in reaction rate at 625°C).

The DTG curves for the reduction of NiO and CoO (Fig. 1, curves 2, 3) show two weight loss regions. Over the entire temperature range studied, the reduction products are metals. The temperatures of the first step,  $\approx 630^\circ\text{C}$  for NiO and  $\approx 730^\circ\text{C}$  for CoO, correlate well with the thermodynamic data for the reactions of these oxide with solid carbon and are attributable to contact reduction on the surface of NiO and CoO. At higher temperatures, the DTG curves of the processes under consideration are indicative of more active reaction owing to the presence of excess carbon. This is associated with the formation of CO gas at temperatures above 750°C, which takes part in the reduction process.

The carbon reduction of  $\text{MoO}_3$  (Fig. 1, curve 4) involves two steps. In the range 460–620°C (maximum in reaction rate at 550°C), we observe the formation of  $\text{MoO}_2$ , which then reacts with  $\text{MoO}_3$  to form  $\text{MoO}_{3-x}$

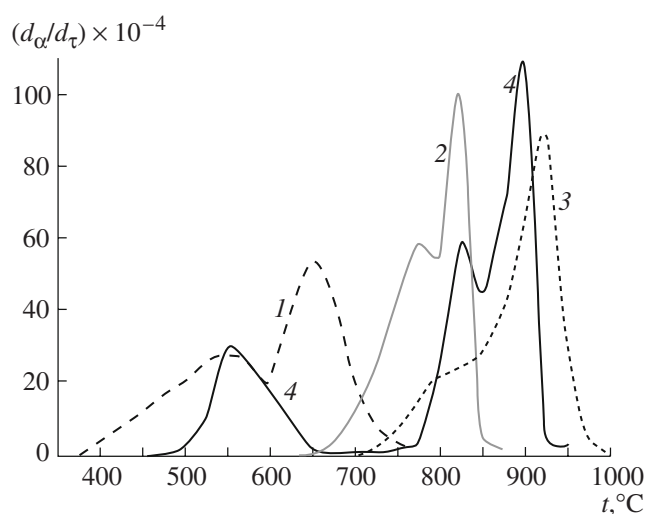


**Fig. 1.** DTG curves for the carbon (50 wt % excess) reduction of oxides: (1) CuO ( $\bar{d} = 3.7\text{ }\mu\text{m}$ ), (2) NiO ( $\bar{d} = 5\text{ }\mu\text{m}$ ), (3) CoO ( $\bar{d} = 4.6\text{ }\mu\text{m}$ ); (4)  $\text{MoO}_3$  ( $\bar{d} = 2.6\text{ }\mu\text{m}$ ).

oxides. The accumulation of intermediate oxides leads to a gradual decrease in reaction rate, and the DTG curve shows a linear portion, corresponding to a negligible reaction rate. Above 775°C, diffusion limitations are partially eliminated owing to the formation of a liquid phase in the reaction zone through the melting of  $\text{Mo}_4\text{O}_{11}$  and  $\text{Mo}_8\text{O}_{23}$ . The second step of reduction (maximum in reaction rate at 820°C) is more active, and its products include Mo and  $\text{Mo}_2\text{C}$ . Since this temperature range corresponds to active CO evolution, the DTG curve shows another maximum in reaction rate, at 910°C, which is due to the excess carbon, like in the case of NiO and CoO.

The onset of the reduction of molybdates in the DTG curves in Fig. 2 (340°C for  $\text{CuMoO}_4$ ,  $\approx 520^\circ\text{C}$  for  $\text{NiMoO}_4$ , and  $\approx 620^\circ\text{C}$  for  $\text{CoMoO}_4$ ) and the weight loss rate correlate with the reactivity of the constituent oxides, which decreases in the order  $\text{CuO} > \text{NiO} > \text{CoO}$  (Fig. 1). In the initial stages of the processes under consideration, the reduction rate notably decreases with decreasing particle size, which seems to be due to the reaction of the oxide surface with carbon. In the DTG curves of  $\text{NiMoO}_4$  and  $\text{CoMoO}_4$ , excess carbon increases the peak at 950°C, where the CO :  $\text{CO}_2$  ratio is sufficient to displace the reaction equilibrium toward CO formation. The formation sequence of reduced and intermediate oxide phases in different temperature ranges was studied in isothermal experiments (table).

The reduction of  $\text{CuMoO}_4$  involves three consecutive steps, evidenced by peaks in its DTG curve (Fig. 2, curve 2). The reaction of  $\text{CuMoO}_4$  with carbon (peak at 405°C) seems to be accompanied by detachment of oxygens from divalent copper atoms, which are thus partially reduced to univalent copper. This is due to the

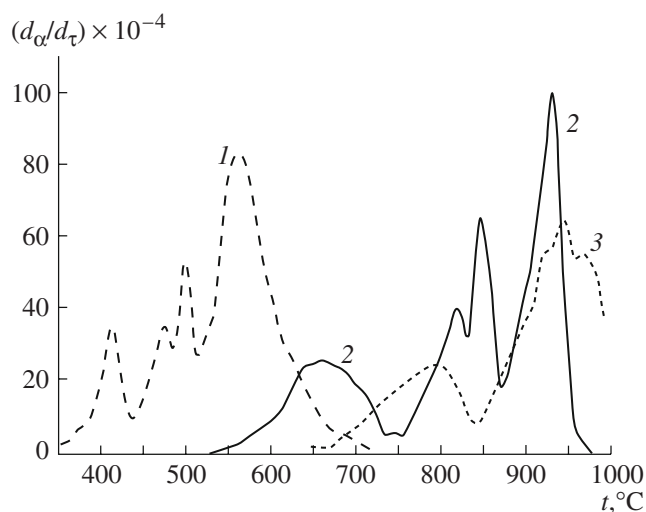


**Fig. 2.** DTG curves for the carbon (50 wt % excess) reduction of molybdates: (1)  $\text{CuMoO}_4$  ( $\bar{d} = 12.7 \mu\text{m}$ ), (2)  $\text{NiMoO}_4$  ( $\bar{d} = 24.1 \mu\text{m}$ ), (3)  $\text{CoMoO}_4$  ( $\bar{d} = 17.7 \mu\text{m}$ ).

higher reactivity of  $\text{CuO}$  compared to  $\text{MoO}_3$  (Fig. 1). We observe the formation of  $\text{Cu}_6\text{Mo}_5\text{O}_{18}$  and  $\text{Cu}_2\text{Mo}_3\text{O}_{10}$ , with no  $\text{Cu}_2\text{O}$  formation. After isothermal heat treatment at  $415^\circ\text{C}$ , the parent molybdate, which consisted of fine ( $d = 2.5 \mu\text{m}$ ) and coarse ( $d = 12.2 \mu\text{m}$ )

Phase composition of the products of carbon reduction of molybdates

$t, ^\circ\text{C}$	$\tau, \text{h}$	$\alpha$	Oxide phases	Reduced phases
$\text{CuMoO}_4 + \text{C}, \bar{d} = 12.2 \mu\text{m}$				
415	3.5	0.18	$\text{Cu}_2\text{Mo}_3\text{O}_{10}$ , $\text{Cu}_6\text{Mo}_5\text{O}_{18}$ ,	Cu
500	2	0.37	$\text{Cu}_2\text{O}$ , $\text{MoO}_2$ , $\text{MoO}_{3-x}$	
600	2	0.49	$\text{MoO}_2$	
$\text{NiMoO}_4 + \text{C}, \bar{d} = 24.1 \mu\text{m}$				
600	2	0.386	$\text{NiMoO}_4$ , $\text{MoO}_{3-x}$ , $\text{MoO}_2$	Ni
850	2	0.79	$\text{NiMoO}_4$	Ni, Mo, $\text{Mo}_2\text{C}$
950	1	0.99		$\text{Ni}_{1-x}\text{Mo}_x$ , $\text{Ni}_4\text{Mo}$ , Mo, $\text{Ni}_x\text{Mo}_y\text{C}_z$ , $\text{Mo}_2\text{C}$
$\text{CoMoO}_4 + \text{C}, \bar{d} = 17.7 \mu\text{m}$				
650	2	0.317	$\text{CoMoO}_4$ , $\text{Co}_2\text{Mo}_3\text{O}_8$ , $\text{CoMoO}_3$	$\text{Co}_7\text{Mo}_6$ , $\text{Co}_3\text{Mo}$ , $\text{Co}_{1-x}\text{Mo}_x$ , Mo, $\text{Co}_x\text{Mo}_y\text{C}_z$ , $\text{Mo}_2\text{C}$
950	1	0.99		

fractions, was not detected by XRD. The presence of two peaks in the DTG curve in the next step of reduction correlates with the endothermic peaks in the DTA curve, whose temperatures,  $455$  and  $505^\circ\text{C}$ , correspond to the congruent melting of  $\text{Cu}_6\text{Mo}_5\text{O}_{18}$  and  $\text{Cu}_2\text{Mo}_3\text{O}_{10}$  [9]. This reaction stage involves phase separation and leads to the formation of  $\text{Cu}_2\text{O}$  (with partial reduction to Cu),  $\text{MoO}_2$ , and  $\text{MoO}_{3-x}$ . The third step, with a peak at  $570^\circ\text{C}$ , is the complete reduction of  $\text{Cu}_2\text{O}$  to Cu.

The reaction of  $\text{NiMoO}_4$  with carbon leads to the formation of Ni metal even in the initial stage, at  $600^\circ\text{C}$  (Fig. 2, curve 2). Some of the  $\text{MoO}_3$  formed is then reduced to  $\text{MoO}_2$  and intermediate molybdenum oxides. Note that, in this temperature range, both NiO and  $\text{MoO}_3$  are capable of being reduced (Fig. 1). The next step, above  $825^\circ\text{C}$ , is accompanied by an endothermic peak in the DTA curve, due to the melting of the intermediate molybdenum oxides. The process is characterized by two maxima in reaction rate, at  $825$  and  $875^\circ\text{C}$ , similar to the peaks in the second step of the reduction of molybdenum(VI) oxide (Fig. 1, curve 4). In this step of the process, fine-particle  $\text{NiMoO}_4$  ( $d = 4.2 \mu\text{m}$ ) is fully reduced to Ni and  $\text{Mo}_2\text{C}$  at  $850^\circ\text{C}$ , while coarser particles ( $d = 24.1 \mu\text{m}$ ) contain the parent molybdate, which reacts with CO as the temperature is raised. The products of  $950^\circ\text{C}$  reduction include, in addition to Ni and Mo, the intermetallic phase  $\text{Ni}_4\text{Mo}$ , a solid solution of molybdenum in nickel  $\text{Ni}_{1-x}\text{Mo}_x$ , XRD peaks in the range  $2\theta = 43^\circ\text{--}44^\circ$ , and a mixed carbide isostructural with  $\text{Ni}_2\text{W}_4\text{C}$ . It seems likely that, during the CO reduction of the molybdate, the rates of nickel and molybdenum formation are comparable to one another, which favors the formation of binary intermetallic compounds.

The carbon reduction of  $\text{CoMoO}_4$  particles via surface reaction starting at  $620^\circ\text{C}$  (Fig. 2, curve 3) occurs with a slow rate (maximum at  $\approx 800^\circ\text{C}$ ). At  $650^\circ\text{C}$ , no metallic Co was detected, while molybdenum was reduced to form the intermediate oxides  $\text{Co}_2\text{Mo}_3\text{O}_8$  and  $\text{CoMoO}_3$  (table), which can be accounted for by the large difference in reactivity between CoO and  $\text{MoO}_3$  at this temperature (Fig. 1). The next step, with a maximum in reaction rate at  $950^\circ\text{C}$ , like in the case of  $\text{NiMoO}_4$ , involves CO evolution. The samples reduced at  $950^\circ\text{C}$  contained intermetallic phases, attesting to coreduction of the metals in the molybdate system:  $\text{Co}_{1-x}\text{Mo}_x$  solid solutions (XRD peaks in the range  $43^\circ\text{--}44^\circ$ ),  $\text{Co}_3\text{Mo}$ ,  $\text{Co}_7\text{Mo}_6$ , and a phase isostructural with the mixed carbide  $\text{Co}_3\text{W}_3\text{C}$ . Also present were Mo and  $\text{Mo}_2\text{C}$ . Note that the particle size of the parent molybdate had no effect on the shape of the DTG curve, but the reaction products of fine-particle  $\text{CoMoO}_4$  ( $\bar{d} = 3.6 \mu\text{m}$ ) contained more carbides, while the reduction of coarse-particle  $\text{CoMoO}_4$  ( $\bar{d} = 17.7 \mu\text{m}$ ) under the same conditions produced, for the most part, metallic phases.

## CONCLUSIONS

The carbothermic reduction of NiO, CoO, CuO, MoO<sub>3</sub>, and the MMoO<sub>4</sub> (M = Ni, Co, Cu) molybdates was studied by TG. In the initial stages of all the processes studied, the surface of molybdate particles reacts with solid carbon. The reduction onset temperatures (340°C for CuMoO<sub>4</sub>, ≈520°C for NiMoO<sub>4</sub>, and ≈620°C for CoMoO<sub>4</sub>) and the sequence of reduction reactions correlate with the reactivity of the constituent oxides, which decreases in the order CuO > MoO<sub>3</sub> > NiO > CoO. The difference in reduction temperature between CuO and CoO in comparison with MoO<sub>3</sub> leads, in the case of CuMoO<sub>4</sub>, to primary reduction of Cu(II) to Cu(I) and the formation of the intermediate compounds Cu<sub>2</sub>Mo<sub>3</sub>O<sub>10</sub> and Cu<sub>6</sub>Mo<sub>5</sub>O<sub>18</sub> and, in the case of CoMoO<sub>4</sub>, to primary reduction of Mo(VI) to Mo(IV) and the formation of Co<sub>2</sub>Mo<sub>3</sub>O<sub>8</sub> and CoMoO<sub>3</sub>. During the congruent melting of Cu<sub>6</sub>Mo<sub>5</sub>O<sub>18</sub> and Cu<sub>2</sub>Mo<sub>3</sub>O<sub>10</sub> (455 and 505°C, respectively), these compounds are reduced by carbon to Cu, MoO<sub>2</sub>, and MoO<sub>3-x</sub>. Co<sub>2</sub>Mo<sub>3</sub>O<sub>8</sub> and CoMoO<sub>3</sub> are nonreactive with carbon but react with CO gas starting at 800°C. The constituent oxides of NiMoO<sub>4</sub> (NiO and MoO<sub>3</sub>) can be reduced by carbon in the same temperature range, leading to the formation of Ni, MoO<sub>2</sub>, and MoO<sub>3-x</sub>, with no intermediate oxide compounds. The present results demonstrate that, even with different reaction paths, the conditions under which only one metallic phase can be obtained favor selective reduction of a mixed oxide. In contrast, in reactions of NiMoO<sub>4</sub> and CoMoO<sub>4</sub> with the CO resulting from the oxidation of carbon, the metals are formed at comparable rates, which favors the formation of metal solid solutions, intermetallic phases, and mixed carbides.

## ACKNOWLEDGMENTS

This work was supported by the Russian Foundation for Basic Research, grant no. 06-02-96000.

## REFERENCES

1. Ban, Z.G. and Shaw, L.L., On the Reaction Sequence of WC-Co Formation an Integrated Mechanical and Thermal Activation Process, *Acta Mater.*, 2001, no. 49, pp. 2933–2939.
2. Barnett, C.J., Burstein, G.T., Kucernak, A.R., and Williams, K.R., Electrocatalytic Activity of Some Carburized Nickel, Tungsten, and Molybdenum Compounds, *Electrochim. Acta*, 1997, vol. 42, no. 15, pp. 2381–2388.
3. Tumarev, A.S., Combined Reduction and Oxidation of Elements, in *Problemy metallurgii* (Current Topics in Metallurgy), Moscow: Akad. Nauk SSSR, 1953, pp. 33–63.
4. Skorokhod, V.V., Solonin, Yu.M., and Uvarova, I.V., *Khimicheskie, diffuzionnye i reologicheskie protsessy v tekhnologii poroshkovykh materialov* (Chemical, Diffusional, and Rheological Processes in Powder Materials Technology), Kiev: Naukova Dumka, 1990.
5. Lebukhova, N.V. and Karpovich, N.F., Carbothermic Reduction of Cobalt and Nickel Tungstates, *Neorg. Mater.*, 2006, vol. 42, no. 3, pp. 357–362 [*Inorg. Mater.* (Engl. Transl.), vol. 42, no. 3, pp. 310–315].
6. Elyutin, V.P., Pavlov, Yu.A., Polyakov, V.P., and Sheboldaev, S.B., *Vzaimodeistvie okislov metallov s uglem* (Reactions of Metal Oxides with Carbon), Moscow: Metallurgiya, 1976.
7. Esin, O.A. and Gel'd, V.P., *Protsessy vysokotemperaturnogo vosstanovleniya* (High-Temperature Reduction Processes), Sverdlovsk: Metallurgizdat, 1957.
8. Samsonov, G.V., Borisova, A.L., Zhidkova, T.G., et al., *Fiziko-khimicheskie svoistva okislov* (Physicochemical Properties of Oxides), Moscow: Metallurgiya, 1978.
9. *Diagrammy sostoyaniya tugoplavkikh oksidov: Spravochnik* (Phase Diagrams of Refractory Oxides: A Handbook), Leningrad: Nauka, 1988, issue 5, part 4, pp. 113–118.